

Analysis and mitigation of measurement uncertainties in the traceability chain for the calibration of photovoltaic devices

This article has been downloaded from IOPscience. Please scroll down to see the full text article.

2009 Meas. Sci. Technol. 20 075101

(<http://iopscience.iop.org/0957-0233/20/7/075101>)

View [the table of contents for this issue](#), or go to the [journal homepage](#) for more

Download details:

IP Address: 38.107.179.213

The article was downloaded on 16/02/2012 at 01:29

Please note that [terms and conditions apply](#).

Analysis and mitigation of measurement uncertainties in the traceability chain for the calibration of photovoltaic devices

Harald Müllejans, Willem Zaaiman and Roberto Galleano

European Commission, Joint Research Centre, Institute for Energy, Renewable Energy Unit,
European Solar Test Installation, Via E Fermi 2749, I-21027 Ispra (Va), Italy

E-mail: harald.muellejans@ec.europa.eu

Received 16 December 2008, in final form 20 March 2009

Published 21 May 2009

Online at stacks.iop.org/MST/20/075101

Abstract

This paper describes the traceability chain for photovoltaic devices and the measurement methods employed to perform the various transfer steps. The measurement uncertainties are analysed in detail based on the accreditation of the European Solar Test Installation (ESTI) for the calibration of photovoltaic devices. The various contributions to the overall uncertainty are critically analysed for various traceability chain options. A major contribution is the uncertainty in the calibration of the primary reference device. The overall measurement uncertainty is reduced using the ESTI reference cell set compared to the traceability from the world photovoltaic scale. For the maximum power of photovoltaic modules, the expanded combined uncertainty is reduced from $\pm 2.6\%$ to below $\pm 2\%$. Recommendations are made on the scope for further reduction of uncertainty and for the best calibration strategy for various PV technologies.

Keywords: calibration, photovoltaics, uncertainty calculation, traceability

1. Introduction

Energy output for photovoltaic devices is commonly related to the declared Watt peak value, i.e. the electrical performance under standard test conditions (STC): the reliability of this value and its associated uncertainty is of crucial importance to manufacturers, operators and investors. Such measurements are carried out either by industry or by PV laboratories. In order to demonstrate its validity, each measurement has to demonstrate an unbroken traceability chain to international primary standards and a calculation of measurement uncertainty for each transfer in the chain. Without either of the two, the measurement is purely indicative and has no legal value, i.e. it would not be acceptable in any kind of dispute.

The traceability of PV reference cells is described in IEC 60904-4 [1], whereas the properties and calibration of PV reference devices are covered by IEC 60904-2 [2]. The measurement of the performance of PV devices is described in IEC 60904-1 [3]. Each of the procedures described in the standards requires one or more measurements. Each

measurement has an associated uncertainty which has to be calculated and documented. In general, measurement uncertainties can be determined following the ISO guide to expression of uncertainty in measurement [4]. In the field of calibration measurement uncertainty is most commonly quoted as expanded uncertainty obtained by multiplying the standard uncertainty by the coverage factor k corresponding to a confidence level of about 95%; normally this factor k is 2. The demonstration of the unbroken traceability chain for all measurement instruments and associated uncertainty calculation is a prime requirement for the accreditation as a calibration laboratory under the ISO 17025 [5] scheme.

In this paper, we describe and evaluate the traceability chain and uncertainty calculation for the measurement of PV devices. Particular attention is being given to the reference devices used commonly to measure the incident irradiance. The traceability chain of instruments such as volt- and ampere-meters or temperature indicators is not explicitly covered, but their contribution to the final uncertainty calculation is considered. The aim of the uncertainty analysis is the identification of those components

which make major contributions. The most promising route to reducing the overall measurement uncertainty is then to work on improvements for these components.

The results presented below represent the current status of the European Solar Test Installation (ESTI), which has been accredited since September 1996 according to the EN45001 standard as the then first photovoltaic testing laboratory. After an ISO 17025 audit in October 2003 ESTI received the status of accredited laboratory for the calibration of PV devices in January 2004 and has since continuously improved its procedures and extended the range of accredited methods.

The procedures are applicable to all kinds of single-junction PV devices including (reference) cells and modules, first (crystalline silicon) and second (thin-film) generation PV devices, provided that suitable connections are provided and response time effects are controlled. The calibration of these devices is currently under high demand and it is the intention of this paper to give laboratories which perform calibrations as well as their clients a deeper understanding of the measurement uncertainties involved. Based on this understanding decisions on measurement strategies and improvements of measurement procedures can be made.

2. Traceability chain

The most important and difficult to obtain traceability chain for the measurement of PV devices is that for the irradiance quantity which is commonly measured by a reference PV device. In this section, a brief outline will be given concerning the traceability of the highest level PV devices (primary references) which is obtained by the transfer from non-PV secondary international standards. In sections 2.2 and 2.3, the transfer from a PV reference device to another PV device is covered.

2.1. Primary references

The highest level of a PV reference cell is a primary reference, also called a primary laboratory reference. The traceability of these devices and possibilities for their calibration are described in IEC 60904-4 [1]. Briefly, there are four methods for transfer traceability from international secondary standards to PV reference cells. At ESTI, three of the four methods have been implemented [6] and accredited. The global sunlight method (GSM) [7, 8] and the direct sunlight method (DSM) [9, 10] transfer the irradiance calibration from two cavity radiometers. The latter takes part regularly (every 5 years, last in 2005) in the International Pyrheliometer Comparison (IPC) [11] where the participating instruments are intercompared against the international primary standard for solar irradiance, the World Radiometric Reference (WRR) [12], composed of a set of cavity radiometers. The solar simulator method (SSM) [6, 13] on the other hand makes reference to the international irradiance scale [14], as represented by a standard lamp. The details of these methods and their associated measurement uncertainty have been described elsewhere [6–10, 13]. Here the uncertainty of the primary reference cell is used as an input to the overall uncertainty calculation for the calibration

of secondary and working references against the primary PV reference. This is the most common situation for the majority of PV testing laboratories that receive the calibration of their primary reference from an external laboratory together with a calibration certificate and associated uncertainty.

It has been shown that the WRR is equivalent to the relevant SI unit within $(0.03 \pm 0.34)\%$ ($k = 2$) [15]. A comparison of primary PV reference cell calibration in the mid-1990s included the DSM and SSM and two other methods. The calibration values attributed to the participating primary reference cells (the so-called World PhotoVoltaic Scale (WPVS)) were taken as the average of the four methods, with an uncertainty of $\pm 1.9\%$ ($k = 2$) [16, 17].

ESTI has based its traceability since then on the WPVS and actively participated in recalibration exercises [18]. The ESTI laboratory is now fully accredited to perform three methods of primary calibration in-house with lower uncertainty [19] and further valid primary calibration measurements from other laboratories have become available over the years. Therefore, the ESTI reference cell set [20] consisting of five full response crystalline silicon reference cells with calibration histories ranging from 5 to 20 years was created. The calibration values assigned to each cell in the ESTI reference cell set are the average of all valid primary calibration results obtained over the lifetime of the cell, as the calibration history proved that the cells are stable. The four primary calibration results contained in the WPVS are considered equally to all other measurements, so that this approach maintains some historical continuity while improving the calibration value considering all available calibration results. The associated uncertainties of the average calibration value are reduced to $\pm 0.64\%$ considering the uncertainties of the primary calibration methods involved and the distribution of all valid calibration results. The uncertainty is incidentally equal to the minimum uncertainty for a primary reference cell calibration at ESTI.

2.2. Secondary references

PV reference cells are commonly used to measure the irradiance of sunlight (either simulated or natural) during the evaluation of the electrical performance of PV devices. Reference cells themselves are PV devices and also have current–voltage (I V) characteristics, which are, however, of limited interest as (within the linearity region) the irradiance is directly proportional to the short circuit current of the reference cell, which is, therefore, the only parameter normally used. In fact, a number of reference cells are shunted, i.e. contain an internal fixed shunt resistance which converts the current to a voltage which is more readily measured. Secondary reference cells are calibrated against primary references according to IEC 60904-2 [2] or IEC 60904-1 [3]. The following sections analyse in detail the uncertainty associated with this transfer step in the daily work in a reference laboratory such as ESTI. The calibrations for other laboratories and industry will normally be carried out using a secondary reference.

2.3. Working references

Working references are PV devices (cells or modules) which will consequently be employed at other laboratories or in industry to perform *IV* measurements. They are calibrated at reference laboratories such as ESTI against secondary references. This transfer is essentially the same as the transfer from primary to secondary, except for the numerical value of the uncertainty of the reference cell. Therefore, the analysis in this paper is also valid for this case. PV modules and (bare) PV cells will be included considering their different sizes in the uncertainty calculation.

3. Measurement methods at ESTI

The principle of all calibrations is that the *IV* characteristics of the PV device to be calibrated are measured by sweeping the device from its short circuit condition (SC) to its open circuit condition (OC) using an electronic load when exposed to (pulsed or continuous) simulated or natural sunlight. Sometimes the device is constantly kept under the SC condition and only the short circuit current is measured. The incident irradiance is measured by the PV reference device, the temperature by appropriate sensors, the current of the PV device by a voltmeter (measuring the potential drop across a calibrated shunt resistor) and the voltage of the device by a voltmeter.

All connections are made with four-point Kelvin probes, as close to the PV device as possible (i.e. on the tabs for bare cells, at the connector for encapsulated cells, at the junction box for modules without cables, at the end of the cables for those with cables). For bare cells, tabs have to be provided, ideally on the back and front surface, but a full backside metallization is acceptable. The approach is to have the cell connectors as they would be when the cell is incorporated in a module. In the absence of such connectors the geometry and type of contacting are crucial and lead to larger uncertainties which are not covered by the present analysis.

3.1. Solar simulators and natural sunlight

ESTI is equipped with two large area pulsed solar simulators (LAPSSs), a continuous solar simulator (CSS) for cell measurements and a measurement set-up to use the natural sunlight, all of which are accredited. Cells up to a size of 12.5 cm × 12.5 cm are measured on the CSS, whereas for larger cell sizes the LAPSSs or the outdoor set-up is used.

3.1.1. Large area pulsed solar simulators. The SpectroLab X25 LAPSS has a light pulse of 2 ms duration with a flat irradiance of 1000 W m⁻², whereas the Pasan IIa has a light pulse with a peak irradiance of 1100 W m⁻² which decays in 20 ms to below 100 W m⁻².

3.1.2. CSS and outdoor. The CSS Wacom WXS 140 Super has two light sources (halogen and xenon) for a continuous irradiance of 1000 W m⁻² over an area of 14 cm × 14 cm. The outdoor set-up uses natural continuous sunlight and can

handle devices up to 2 m × 2 m inside a thermally isolated box with sliding doors.

3.2. Common instruments and procedures

3.2.1. Data acquisition system. The incident irradiance (measured as the short circuit current of the reference cell which is transformed to a voltage output by a transimpedance amplifier), the voltage across the PV device (measured with two of the four Kelvin probes) and its current (as a voltage across the shunt in the shunt box) are acquired simultaneously by a four-channel digital storage oscilloscope with a sampling frequency of 1 MHz and 12 bit digitization. Typically for each measurement a total of 5000 points per channel are acquired of which 1500 points are for the actual *IV* curve. The data are transferred via the GBIP interface to a PC after the end of data acquisition.

3.2.2. Electronic load and shunt box. The electronic load is a four-quadrant bipolar power supply (KEPCO), which is driven in voltage mode by a function generator such that the PV device is swept from a slightly negative potential to beyond the open circuit voltage, thereby including both (current and voltage) zero crossings. The current passes through a shunt box, which contains a number of software selectable relay-switched calibrated shunt resistors (to cover various current ranges with an optimum voltage for the data acquisition system).

This system is common to the Pasan, Wacom and outdoor set-up. It could also easily be used on the Spectrolab (mobile Pasan load); however, on this simulator the original electronic load is still used, together with the data acquisition system described above. The electronic load is one quadrant, but has a sufficient range to cover the zero crossings. It also incorporates the calibrated shunt resistors for current measurement.

3.2.3. Transimpedance amplifier for reference cells. The reference cell is connected to in-house constructed transimpedance amplifiers, which maintain the reference cell under short circuit condition while the current can be measured as a voltage drop across a calibrated high stability 1 Ω shunt resistor.

3.2.4. Temperature sensors. The temperatures of the reference device and the PV device are measured by PT100 sensors attached to the centre back of the device with metal tape. Both temperatures are read by a dual channel temperature recorder and transferred by an RS232 interface to the PC. If available, internal temperature sensors (also RTD) (normally for reference cells) are used as an additional control. Thermocouples are not used for temperature measurement at ESTI.

3.2.5. Reference cell. Any primary or secondary reference of the laboratory is used at a temperature of (25.0 ± 0.1) °C. This is achieved on the LAPSSs by controlling the environment, on the CSS by mounting the reference cell on a water cooled plate and outdoor by means of a Peltier cooled plate.

3.2.6. *Intermediate instruments.* Each set-up has a number of intermediate instruments such as four-quadrant bipolar power supply (KEPCO—except Spectrolab), function generator and PC with in-house developed software. Intermediate instruments are essential for the execution of the test, but they themselves do not give any measurement results.

3.2.7. *Point by point.* The irradiance (from the reference device) as well as voltage and current of the module are acquired simultaneously point by point. On the CSS, due to the limited size of the illuminated area, the irradiance is measured with the reference device before and after each *IV* characteristic in the centre of the measurement area. The average irradiance is taken as the actual irradiance if the two measurements differ by less than 0.2%.

3.3. Differences in set-up and procedures

3.3.1. *Sweep time.* Typical sweep times are 1–1.5 m for the LAPSSs, and 1 s for the CSS and outdoor.

3.3.2. *Temperature range and non-uniformity.* The temperature of the devices indoor is kept at $(25 \pm 0.1)^\circ\text{C}$ achieved through the controlled environment for the LAPSSs and a water cooled mounting plate for the Wacom. The estimated temperature non-uniformity for module indoors is 0.5°C whereas for outdoors it is 3°C .

3.3.3. *Spatial non-uniformity and device alignment and orientation.* The spatial non-uniformity of the CSS is measured across the illuminated area and used in the calculation. For natural sunlight it is neglected altogether. For the LAPSSs it is calculated based on the assumption of a point source (which has been shown to be a good approximation [21]). The lamp to target distances of the two systems are 12.5 m and 7 m respectively. For the uncertainty calculation a $\pm 1\%$ non-uniformity is assumed, because the respective areas cover most of the current PV module sizes.

Furthermore, the orientation towards the lamp for the reference cell side by side to the device under test is considered for the LAPSSs and a deviation of $1\text{--}3^\circ$ from co-planarity between both devices for all systems is estimated.

3.3.4. *Spectral mismatch correction.* The calculation of the spectral mismatch [22] depends on the spectral response of the device under test and the reference device as well as the spectral irradiance during *IV* characterization and the reference spectral irradiance (IEC 60904-3) [23]. The former three have associated uncertainties which translate into an uncertainty of the spectral mismatch correction. From the calculations (not reported here) the major component is the uncertainty of the spectral irradiance of the (simulated) sunlight. This is much higher for the LAPSS because of the difficulty in measuring it, whereas for the CSS it is measured with a spectroradiometer traceable to the international irradiance scale via a standard lamp.

3.4. *IV* curve translation according to IEC 60891

The *IV* characteristics are measured near the temperature of 25°C (as required under standard test conditions). Corrections of the measured *IV* curves with respect to temperature are not made (i.e. temperature coefficients are not required). The deviation and its uncertainty from the temperature of 25°C are considered as an uncertainty component. The measurements are also performed at irradiances near 1000 W m^{-2} (STC) with a typical deviation of less than $\pm 2\%$ from this value (class A simulator). As a consequence, the correction of the *IV* characteristics according to IEC 60891 [24] is small and the effect of the module series resistance can be neglected.

3.5. Spectral response (SR)

The spectral response of PV devices can be measured at ESTI with two set-ups using quasi-monochromatic light obtained from xenon light sources with suitable bandpass filters [25, 26]. The set-up for modules uses the Pasan LAPSS, which produces a single flash illuminating the entire device up to the size of $1.5\text{ m} \times 2.0\text{ m}$. The short circuit current is measured with a transimpedance amplifier. The set-up for cells (up to $30\text{ cm} \times 30\text{ cm}$) obtains chopped monochromatic light from a continuous xenon light source and measures the induced short circuit current by a lock-in technique. In both set-ups the resulting short circuit current in a calibrated reference device placed next to the device is measured simultaneously.

The spectral mismatch is calculated [22] from the measured SR of the device [27], the SR of the reference used for the *IV* measurement and the spectral irradiance during the *IV* determination, and the *IV* characteristic is corrected accordingly.

4. Calculation of measurement uncertainties

4.1. Definitions and assumptions

The maximum power under standard test conditions ($P_{\text{max-STC}}$) is obtained as

$$P_{\text{max-STC}} = I_{\text{sc-STC}}^* V_{\text{oc-STC}}^* \text{FF}(\text{fill factor}). \quad (1)$$

The expanded ($k = 2$) combined measurement uncertainty for $P_{\text{max-STC}}$ can be determined as

$$U_{P_{\text{max-STC}}} = (U(I_{\text{sc-STC}})^2 + U(V_{\text{oc-STC}})^2 + U(\text{FF})^2)^{1/2} \quad (2)$$

with $U(I_{\text{sc-STC}})$ the expanded combined uncertainty for I_{sc} , $U(V_{\text{oc-STC}})$ the expanded combined uncertainty for V_{oc} and $U(\text{FF})$ the expanded combined uncertainty for FF.

For the reference device and device under test the following assumptions are made.

$$\text{Temperature coefficient for current: } 500\text{ ppm }^\circ\text{C}^{-1}; \quad (3)$$

$$\text{temperature coefficient for voltage: } -0.33\% \text{ }^\circ\text{C}^{-1}; \quad (4)$$

$$\text{diode coefficient: } D * [\ln(I_{\text{rr,m}}/I_{\text{rr,corr}})]; \quad (5)$$

$$D = 5.3\% \text{ of } V_{\text{oc}} \text{ (with } 600\text{ mV for } V_{\text{oc}}), \quad (6)$$

Table 1. Uncertainty components considered for the calibration of PV devices. It is indicated whether the calculations are common (C), similar (S) or different (D) and reference is made to the tables below for the components and their combined effect.

Uncertainty	Component	C	S	D	Component	Combined
Electrical	Data acquisition system	X			2a	2d
	Shunt (determination of the device under test current)	X			2b	
	Transimpedance amplifier for the reference device	X			2c	
Temperature	Temperature indicator and sensor (PT100)	X			3a	3d
	Temperature range during the characterization		X		3b	
	Temperature non-uniformity (only for modules)		X		3c	
Optical	Spatial non-uniformity			X	4a	4d
	Orientation of the device under test and the reference device			X	4b	
	Alignment of the device under test and the reference device		X		4c	
Reference cell	Reference cell responsivity	X			5a	5d
	Spectral mismatch correction		X		5b	
	Reference cell drift	X			5c	
Fill factor	Variations on the LAPSS and outdoor		X		6a	6c
	Variations on the Wacom		X		6b	

where $I_{tr,m}$ is the measured irradiance and $I_{tr,corr}$ is the corrected irradiance, normally 1000 W m^{-2} .

For all the instrumentation (temperature reading devices, shunts and data acquisition system), the temperature dependence is neglected as the temperature of the instruments during measurements is within their operating range.

The tables for the uncertainty components list the standard ($k = 1$) uncertainties expressed in % with the following symbols:

uH	Standard uncertainty for irradiance
uV	Standard uncertainty for voltage
uI	Standard uncertainty for current
uFF	Standard uncertainty for fill factor

The divisor of $\sqrt{3}$ is used for components with a rectangular probability distribution. All uncertainty components are expressed in % with three decimal places, except for the final expanded ($k = 2$) combined uncertainty with two decimal places rounded.

The uncertainty for the FF depends on the electrical connections and is not dependent on irradiance, current and voltage measurements and will, therefore, be considered separately at the end.

4.2. Identification of uncertainty contributions

The following contributions to measurement uncertainty have been identified (table 1). For each component it is indicated whether it is common (C) to all measurement set-ups (same principle and same numerical value), similar (S) because they are based on the same principle, but different numerical values have to be used or different (D).

4.3. Electrical uncertainty

4.3.1. Data acquisition. The value listed by the manufacturer is $\pm 0.25\%$ full scale which transfers to a standard uncertainty

Table 2a. Data acquisition system UC.

	uH	uV	uI
DAS	± 0.097	± 0.097	± 0.137

Table 2b. Shunt UC.

	uH	uV	uI
Shunts	± 0.000	± 0.000	± 0.115

Table 2c. Reference cell TIA UC.

	uH	uV	uI
Reference cell TIA	± 0.058	± 0.003	± 0.058

Table 2d. Combined electrical standard uncertainty.

	uH	uV	uI
Combined electrical UC	± 0.113	± 0.097	± 0.188

of $\pm 0.097\%$ assuming a 99% confidence level ($k = 2.586$) (table 2a). Measurement ranges are selected in order to have input signal values around two thirds of the full scale. The uncertainties for the measured current have two contributions, one from the raw current measurement and one from the irradiance measurement, because the current is directly proportional to the irradiance and measurements are corrected to a defined irradiance.

4.3.2. Shunts. Each instrument has a dedicated shunt box containing several shunts which are verified yearly. The data analysis is based on the nominal shunt value. Therefore, the deviation from the nominal value is considered as a bias error. Based on several years of data the maximum bias error is $\pm 0.20\%$ with a rectangular distribution (table 2b). Only the current of a device is affected.

Table 3a. Temperature indicator UC.

	uH	uV	uI
Temperature indicator	± 0.003	± 0.019	± 0.004

Table 3b. Temperature deviation UC.

Temperature deviation	uH	uV	uI
Indoor	± 0.003	± 0.019	± 0.004
Outdoor	± 0.058	± 0.381	± 0.082

Table 3c. Temperature non-uniformity UC (only for modules).

Temperature non-uniformity	uH	uV	uI
Indoor (modules)	± 0.000	± 0.095	± 0.014
Outdoor (modules)	± 0.000	± 0.572	± 0.087

Table 3d. Combined temperature standard uncertainty (for cells and modules).

Combined temperature UC	uH	uV	uI
Indoor (cells)	± 0.004	± 0.027	± 0.006
Outdoor (cells)	± 0.058	± 0.382	± 0.082
Indoor (modules)	± 0.004	± 0.099	± 0.016
Outdoor (modules)	± 0.058	± 0.687	± 0.119

4.3.3. Reference cell transimpedance amplifier. The effect of the temperature drift ($4 \mu\text{V } ^\circ\text{C}^{-1}$) and the offset voltage (0.8 mV maximum) is negligible on the irradiance signal, because due to the slope (dI/dV) near I_{sc} of $\geq 5 \text{ mS}$ the effect of 0.8 mV offset is only $4 \mu\text{A}$ (absolute) on a typical signal $> 100 \text{ mA}$, i.e. $< 0.004\%$.

The uncertainty of $\pm 0.10\%$ in the shunt of the transimpedance amplifier with rectangular distribution results in a 1σ uncertainty of $\pm 0.058\%$ and $uV = D \ln(H_m + uH)/H_{1000}$ (4)–(6) (table 2c).

On the basis of the above results, the combined electrical standard uncertainty (u_{CES}) is calculated for the three simulators (table 2d).

4.4. Temperature uncertainty

The temperature range during calibration is $(25.0 \pm 0.1) ^\circ\text{C}$ under the LAPSS and Wacom and $(25.0 \pm 2.0) ^\circ\text{C}$ under outdoor conditions. The temperature non-uniformity within a module is estimated to be within $0.5 ^\circ\text{C}$ indoor and $3 ^\circ\text{C}$ outdoor. For cells this component is neglected. All distributions are rectangular. The following analysis applies to the PT100 temperature sensors in use at ESTI. Different temperature sensor types (e.g. thermocouples) may lead to different measurement uncertainties.

4.4.1. Temperature indicators. The temperature indicators are specified (manufacturer data) with an uncertainty of $\pm 0.1 ^\circ\text{C}$. The temperature indicators are verified and calibrated in-house and the maximum deviation of all the indicators in the range $(25.0 \pm 2.0) ^\circ\text{C}$ is less than $\pm 0.1 ^\circ\text{C}$. This results in a

1σ uncertainty of $\pm 0.058 ^\circ\text{C}$ which propagates (equations (3)–(6)) via the temperature coefficient of the irradiance, current and voltage measurements as follows (table 3a):

$$\text{irradiance: } 500 \text{ ppm } ^\circ\text{C}^{-1} \times \pm 0.058 ^\circ\text{C} = \pm 29 \text{ ppm} \\ = \pm 0.0029\%,$$

$$\text{voltage: } 0.33\% ^\circ\text{C}^{-1} \times \pm 0.058 ^\circ\text{C} = \pm 0.019\% \text{ and}$$

$$\text{current: } 500 \text{ ppm } ^\circ\text{C}^{-1} \times ((\pm 0.058 ^\circ\text{C})^2 + (\pm 0.058 ^\circ\text{C})^2)^{1/2} \\ = \pm 41 \text{ ppm} = \pm 0.0041\%.$$

4.4.2. Temperature deviation during measurement. The deviation of device temperature is treated as uncertainty as the IV characteristics are not corrected for temperature. The results of the temperature indicator calculation section 4.4.1 can be copied as the deviation is the same ($\pm 0.1 ^\circ\text{C}$).

For outdoor measurements the calculation is done with the larger deviation of $2 ^\circ\text{C}$ giving a 1σ uncertainty of $\pm 1.15 ^\circ\text{C}$ (table 3b).

4.4.3. Temperature non-uniformity (only for modules). Only for modules is the temperature non-uniformity taken into account. The temperature effect is neglected for the reference cell signal and also for the device under test whenever it is a cell. As the measurements are performed in a temperature-controlled environment, a maximum temperature non-uniformity of $\pm 0.5 ^\circ\text{C}$ is assumed indoors leading to a 1σ uncertainty of $\pm 0.29 ^\circ\text{C}$. Outdoors a temperature non-uniformity of $\pm 3.0 ^\circ\text{C}$ is assumed yielding a 1σ uncertainty of $\pm 1.73 ^\circ\text{C}$. Analogous calculation gives values in table 3c.

On the basis of the above results, the combined temperature standard uncertainty (u_{CTS}) for modules and cells is calculated (table 3d).

4.5. Optical uncertainty

4.5.1. Spatial non-uniformity. The area in the target plane for a $\pm 1\%$ non-uniformity is calculated under the assumption of a point source for the SpectroLab LAPSS and Pasan LAPSS [21] with 12.5 m and 7 m lamp-to-target distances respectively and the light intensity following the $1/R^2$ rule (see figure 1).

The $\pm 1\%$ $L1$ non-uniformity locations on the target plane are calculated as $L1 = (1.02)^{1/2} \times L$; therefore, $r1 = [(L1)^2 - L^2]^{1/2}$. For the SpectroLab LAPSS ($L = 12.5 \text{ m}$) this results in $r1 = 1.77 \text{ m}$ and for the Pasan ($L = 7 \text{ m}$) in $r1 = 0.99 \text{ m}$. As most of the modules are smaller than 2 m in diagonal, the $\pm 1\%$ non-uniformity is used for the calculations (with divisor $\sqrt{3}$ assuming a rectangular distribution).

For the Wacom simulator the non-uniformity of the irradiance was measured using two $2 \text{ cm} \times 2 \text{ cm}$ cells. One cell is kept at the centre of the measurement area to account for temporal lamp intensity variations while the second cell is moved to various positions in the measurement area to map the spatial irradiance variation. For cells of the same dimensions as the reference cell, the residual uncertainty due to reproducible positioning is considered, whereas for cells with an active area larger than that of the reference cell, the spatial non-uniformity is integrated over the active area and

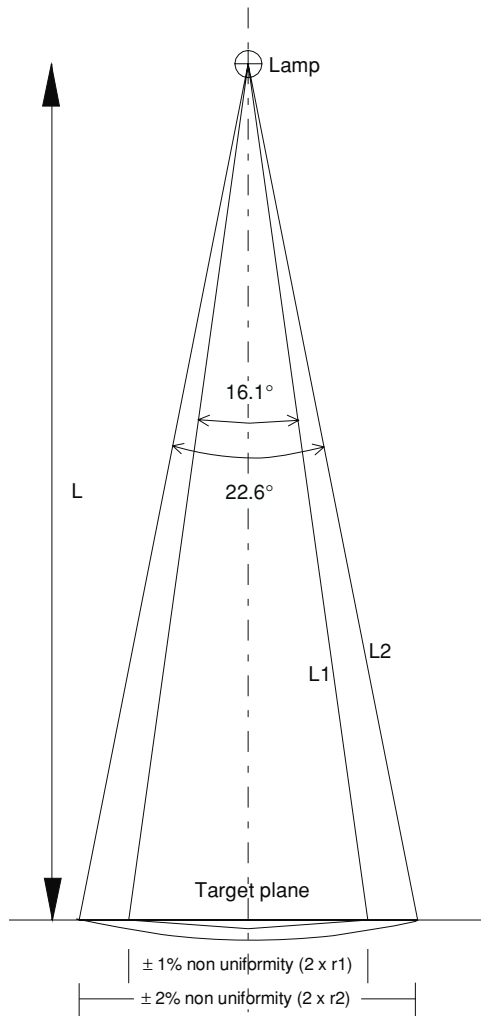


Figure 1. Spatial non-uniformity.

corrected for. In both cases the remaining uncertainty due to non-uniformity is $\pm 0.4\%$ with a rectangular distribution.

The voltage uncertainty is calculated according to equations (5) and (6).

For the outdoor set-up perfect uniformity of the natural sunlight is assumed. For cells on both LAPSSs the non-uniformity is considered to be negligible.

4.5.2. Orientation. The orientation of the devices with respect to the beam is only considered for modules on the LAPSSs. (For the Wacom and outdoor, or cells on the LAPSS a perfectly parallel beam is assumed.) Figure 1 shows that the irradiance illuminates the reference cell off-axis with a maximum angle of incidence (for $\pm 1\%$ non-uniformity) of $16.1^\circ/2 = 8.05^\circ$ due to the positioning of the reference cell besides the module. With a 99% confidence limit, the 1σ would be 3.11° ($k = 2.586$ assuming a Gaussian distribution). The effect on the irradiance is $(1 - \cos(3.11^\circ)) = 0.148\%$ (table 4b).

4.5.3. Misalignment. Assuming a maximal misalignment of 3° between the device under test and the reference cell for both LAPSSs and outdoor, the 1σ would be 1.73° . The effect on

Table 4a. Spatial non-uniformity UC (only for cells).

Non-uniformity	uH	uV	uI
LAPSS (modules)	± 0.577	± 0.031	± 0.577
Wacom CSS (cells)	± 0.231	± 0.012	± 0.231
LAPSS (cells)/outdoor (cells and modules)	± 0.000	± 0.000	± 0.000

Table 4b. Orientation UC (only for modules).

Orientation	uH	uV	uI
LAPSS (modules)	± 0.148	± 0.008	± 0.148
LAPSS (cells)/Wacom CSS (cells)/outdoor (cells and modules)	± 0.000	± 0.000	± 0.000

Table 4c. Misalignment UC.

Misalignment	uH	uV	uI
LAPSS/outdoor	± 0.046	± 0.002	± 0.046
Wacom CSS	± 0.005	± 0.000	± 0.005

Table 4d. Combined optical standard uncertainty.

Combined optical UC	uH	uV	uI
LAPSS (modules)	± 0.598	± 0.032	± 0.598
LAPSS (cells)/outdoor (cells and modules)	± 0.046	± 0.002	± 0.046
Wacom CSS (cells)	± 0.231	± 0.012	± 0.231

the irradiance and current = $[1 - \cos(1.73^\circ)] = \pm 0.046\%$. The effect on the voltage is $\pm 0.002\%$. For the Wacom CSS the misalignment is at most 1° . The results are shown in table 4(c).

On the basis of the above results the combined optical standard uncertainty (u_{COS}) for cells is calculated for the three simulators (table 4d).

4.6. Reference cell uncertainty

4.6.1. Reference cell responsivity. The reported [16] uncertainty of WPVS cells is a 2σ value of $\pm 1.9\%$, i.e. a 1σ uncertainty of $\pm 0.95\%$ for irradiance and current. For voltage this yields $\pm 0.05\%$ according to equations (5) and (6). The smallest possible uncertainty for primary calibration is $\pm 0.32\%$ (1σ) [19] (table 5a).

4.6.2. Determination of spectral mismatch correction. The 1σ standard uncertainty of the spectral mismatch correction is stated as $\pm 0.52\%$ in UC04 [28] for measurements on the LAPSSs. For measurements on the CSS or outdoor the respective value is $\pm 0.19\%$ (table 5b) [29]. The calculation of the uncertainty for mismatch correction is based on the previous work [30, 31] and explained in [6]. Briefly it has been shown in [31] that the uncertainty contribution to the mismatch correction is ten times less than the uncertainty in relative spectral response and in spectral irradiance. The standard uncertainty for the SR of the reference cell and the devices to be calibrated is of the same order of magnitude as

Table 5a. Reference device UC.

Reference cell responsivity	uH	uV	uI
WPVS	±0.950	±0.050	±0.950
Primary calibration/ESTI reference cell set	±0.320	±0.017	±0.320

Table 5b. Spectral mismatch UC.

Spectral mismatch	uH	uV	uI
LAPSS	±0.000	±0.000	±0.520
CSS and outdoor	±0.000	±0.000	±0.190

Table 5c. Reference cell drift—instability UC.

	uH	uV	uI
Reference cell drift	±0.110	±0.006	±0.110

Table 5d. Combined reference device standard uncertainty.

Combined reference cell UC	uH	uV	uI
WPVS—LAPSS	±0.956	±0.050	±1.089
Primary calibration/ESTI reference cell set—LAPSS	±0.338	±0.018	±0.620
WPVS—CSS/outdoor	±0.956	±0.050	±0.975
Primary calibration/ESTI reference cell set—CSS/outdoor	±0.338	±0.018	±0.388

the standard uncertainty in the short circuit current, i.e. around 1%, which applies to both cells and modules. The standard uncertainty for the spectral irradiances of a CSS or natural sunlight can be measured with a spectroradiometer with a standard uncertainty of 1.12% whereas for a pulsed simulator this value increases to 5%. Summing the squares of these three contributions and considering the reduction factor of 10 lead to the values in table 5b.

4.6.3. Reference cell drift—instability. The results of the yearly verifications of the reference devices show typical drift/instability of $\pm(0.19\% \pm 0.05\%)$. Assuming a rectangular distribution yields the values in table 5c.

On the basis of the above results, the combined reference device standard uncertainty (u_{CDS}) for cells and modules is calculated for the three simulators and presented in table 5d.

4.7. Fill factor uncertainty

To determine the effect of the software, cabling and connections on the fill factor, measured data of SpectroLab and Pasan are used. Data for outdoor measurements are not available yet, but the same result is assumed as the same four-wire connection method is used.

Various module types (of reference modules for module qualification testing) have been measured repeatedly with disconnecting and reconnecting of the modules, often with several days in between measurements (table 6a). We assume that all sources of variations in the fill factor occur randomly.

Table 6a. Experimental determination of variations in fill factor on SpectroLab and Pasan. The same values are assumed for measurements on the outdoor set-up based on the identical connection method.

	Number of measurements	Average FF	Standard deviation ($k = 1$) in FF	
BO01	13	0.7338	±0.0016	±0.22%
CE01	13	0.6832	±0.0028	±0.40%
KD01	12	0.7063	±0.0014	±0.19%
NF01	11	0.6433	±0.0049	±0.76%
NG01	10	0.6972	±0.0045	±0.64%
PF01	23	0.6889	±0.0010	±0.15%
SG01	7	0.6967	±0.0020	±0.28%
TC01	9	0.6981	±0.0039	±0.55%
VE01	18	0.7302	±0.0018	±0.24%
WB01	7	0.6713	±0.0031	±0.46%
XG01	14	0.6896	±0.0021	±0.30%
ZC01	11	0.7178	±0.0010	±0.14%
ZG01	10	0.6925	±0.0020	±0.28%

Table 6b. Experimental determination of variations in fill factor on the Wacom.

Device ID	Number of measurements	Average FF	Standard deviation ($k = 1$) in FF	
CI511	6	0.7054	±0.0045	±0.64%
IM501	6	0.7451	±0.0014	±0.19%
IM502	5	0.7444	±0.0037	±0.50%
IM505	9	0.7776	±0.0059	±0.76%
IM506	9	0.7806	±0.0042	±0.54%
TG011	6	0.7298	±0.0014	±0.19%
UK509	6	0.7761	±0.0027	±0.35%

Table 6c. Combined fill factor standard uncertainty.

Fill factor UC	uFF
LAPSSs and outdoor	±0.36
Wacom CSS	±0.45

The standard deviation is then an acceptable metric for the uncertainty of a single measurement.

For the Wacom simulator a similar data set is available but over a shorter time span (table 6b). The values are higher because the contacts to bare cells are less reproducible than those to modules which utilize quick connectors or screw connections in the junction box.

The average of the last column values in tables 6a and 6b is used for the standard ($k = 1$) uncertainty for the fill factor determination.

4.8. Expanded combined uncertainty

With the combined standard uncertainties available the uncertainties in the components for formula (2) can be determined. As the irradiance contribution to voltage and current is already considered in tables 2–6, the combined uncertainty can directly be calculated from the latter two columns adding the uncertainty of FF. The expanded combined uncertainty is calculated for the various measurement set-ups and device types. Two different reference cell uncertainty/traceability chains are considered as well as the repeatability of the measurements (tables 7–9).

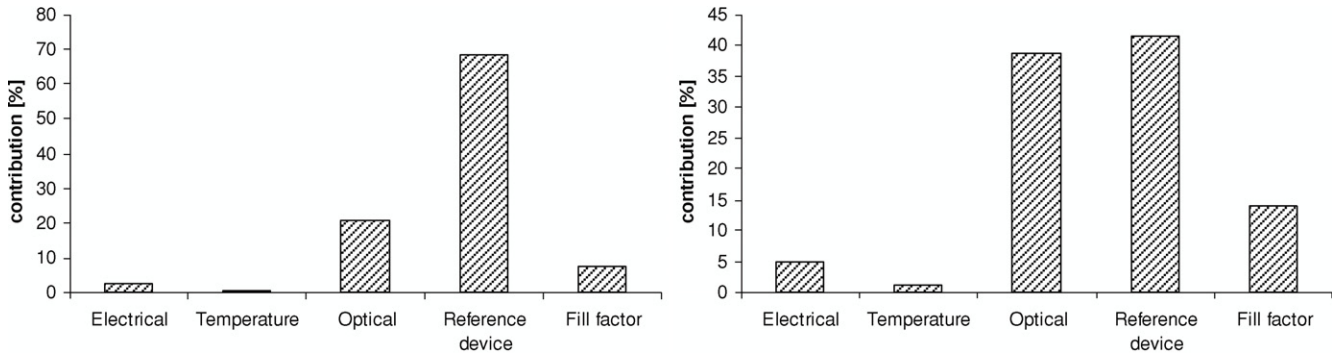


Figure 2. Relative contributions to combined uncertainty of maximum power for WPVS traceability (left) and the internal primary calibration/ESTI reference cell set (right) for modules measured on LAPSS. The total measurement uncertainties are $\pm 2.62\%$ and $\pm 1.96\%$ respectively.

Table 7. Combined I_{sc} , V_{oc} and P_{max} expanded uncertainty in % based on the WPVS reference cell.

System	Cells			Modules		
	I_{sc}	V_{oc}	P_{max}	I_{sc}	V_{oc}	P_{max}
Spectrolab + Pasan LAPSS	± 2.21	± 0.22	± 2.33	± 2.51	± 0.30	± 2.62
Wacom	± 2.04	± 0.23	± 2.21	NA	NA	NA
Outdoor	± 1.99	± 0.79	± 2.27	± 2.00	± 1.39	± 2.55

Table 8. Minimum achievable combined I_{sc} , V_{oc} and P_{max} expanded uncertainty in % based on the accredited primary reference cell calibration/ESTI reference cell set at ESTI.

System	Cells			Modules		
	I_{sc}	V_{oc}	P_{max}	I_{sc}	V_{oc}	P_{max}
Spectrolab + Pasan LAPSS	± 1.30	± 0.20	± 1.50	± 1.76	± 0.29	± 1.96
Wacom	± 0.98	± 0.21	± 1.35	NA	NA	NA
Outdoor	± 0.88	± 0.79	± 1.38	± 0.90	± 1.39	± 1.81

Table 9. Combined I_{sc} , V_{oc} and P_{max} expanded uncertainty in % for repeatability (based on the same device against the same reference cell) as applicable to module qualification testing and the verification of calibration stability.

System	Cells			Modules		
	I_{sc}	V_{oc}	P_{max}	I_{sc}	V_{oc}	P_{max}
Spectrolab + Pasan LAPSS	± 0.45	± 0.20	± 0.87	± 1.27	± 0.28	± 1.51
Wacom	± 0.64	± 0.20	± 1.12	NA	NA	NA
Outdoor	± 0.47	± 0.79	± 1.17	± 0.50	± 1.39	± 1.65

Note. The values for outdoor are based on the assumption of the same spectrum for all measurements. Spectral variations might potentially change the spectral mismatch and lead to a higher variation in the repeatability.

5. Discussion

5.1. Contribution of various components

The relative importance of the various uncertainty contributions for the values presented in tables 7 and 8 shows which component should be improved in order to reduce the overall uncertainty. As an example the case of a module calibration on the LAPSSs against the two possible traceability chains is examined. In the case of using a WPVS traceable reference cell the relative contributions to the uncertainty in peak power of the module are 69% from the reference device, 21% from the optical uncertainty and 7% from cabling/FF (other contributions are minor to add up to a total of 100%) whereas the use of a primary reference with a lower uncertainty

changes the situation somewhat, the reference device and optical uncertainty now each contributing about 40% and the cabling 14% (other contributions adding to 100%) (figure 2). For outdoor calibration (not shown) the optical uncertainty is negligible (due to the collimated sunlight), but the temperature uncertainty contributes about 60% to the overall uncertainty in maximum power.

The uncertainty of the reference cell is always a major component, but can be reduced by primary calibration with respect to WPVS. For the calibration on the LAPSSs the optical uncertainty is the second most important contribution and cabling the third. For outdoor the optical uncertainty is replaced by the temperature uncertainty. As neither the uncertainty of calibration for primary reference cells nor of

Table 10. Comparison of the achievable combined uncertainty in I_{sc} for reference cell calibration, primary calibration, WPVS and secondary calibration against both references in %.

	Primary reference cell calibration	Calibration of the secondary reference cell against the primary reference cell		Calibration of the working reference against the secondary reference cell	
		LAPSS	Wacom	Cells Wacom	Modules LAPSS
	I_{sc}	I_{sc}	I_{sc}	I_{sc}	P_{max}
WPVS	± 1.90	± 2.21	± 2.04	± 2.17	± 2.71
GSM\ESTI reference cell set	± 0.64	± 1.30	± 0.98	± 1.23	± 2.05
SSM	± 2.26	± 2.53	± 2.38	± 2.49	± 3.00

the cabling is easily reducible, the two remaining aspects to address are the spatial non-uniformity for LAPSS and temperature control for the outdoor set-up.

5.2. Calibration of references

The prime example is the in-house calibration of a secondary reference (normally the same size and type) against a primary reference. The important parameter is the short circuit current I_{sc} , as it is used to determine the irradiance intensities in further measurements. Starting with a WPVS reference cell the achievable uncertainty on a secondary cell is $\pm 2.0\%$ (Wacom) and $\pm 2.2\%$ (LAPSSs) whereas using an in-house primary calibrated reference cell or the ESTI reference cell set it is $\pm 0.98\%$ and $\pm 1.30\%$ respectively (table 10). The lower uncertainties are achieved for the CSS, as the spectral irradiance can be determined with lower uncertainty than for the LAPSSs, and therefore, less uncertainty in the spectral mismatch correction leads to the lower overall uncertainty. The calculations are conservative as they contain the spatial non-uniformity which could be neglected if both devices are of the same size and positioned identically (consecutively).

If in a further step a working reference cell is calibrated against a secondary reference, the uncertainty can be calculated analogously, using the uncertainty of the secondary as an input parameter in the calculation. Using a secondary reference with an uncertainty of $\pm 0.98\%$, the working reference has an uncertainty of $\pm 1.23\%$ if calibrated on the Wacom. This value is significantly less than that of any secondary reference calibrated against the WPVS. It is also smaller than the uncertainty of the primary calibration via the solar simulator method [6]. Other laboratories would then be able to calibrate further references with an uncertainty of $\pm 1.5\%$ if they have instruments and procedures similar to those in place at ESTI.

For PV modules as working references, the uncertainties are somewhat larger (table 10). Based on a secondary reference cell with $UC = \pm 0.98\%$, I_{sc} of the module would have a $\pm 1.91\%$ uncertainty and the maximum power $\pm 2.05\%$ (not shown) when calibrated with the LAPSSs. For an outdoor calibration the uncertainty of I_{sc} would be reduced to $\pm 1.17\%$, as the major contribution on the LAPSS is the non-uniformity, which is eliminated outdoor. However, due to larger temperature uncertainties, the uncertainty of P_{max} is $\pm 1.98\%$, i.e. only slightly below that of the indoor result.

If further modules are calibrated against this reference module, the short circuit current of the reference module and

its uncertainty are relevant. Therefore, the outdoor calibration of the reference module is to be preferred.

Given that the increase in uncertainty is limited if proper transfer procedures are used such as those described here, a reference laboratory should have a set of primary reference cells which are calibrated by primary methods and used for international intercomparisons and transfer to a number of secondary references. At ESTI we have, therefore, established the ESTI reference cell set, which currently contains five primary reference cells. Their calibration value and its uncertainty are based on their entire calibration history of valid primary calibrations. The secondary references are then used in daily work for transfer to working standards in other laboratories and PV industries. The latter have the choice of using the working references directly (and regularly recalibrating them) or performing a further in-house transfer to other working standards to be used in daily routine. The choice will depend on the frequency of use of the reference. In any case the transfer and measurement procedure should be documented and an associated uncertainty calculation should be performed.

5.3. Calibration of thin-film devices

The calculations above have been made with conventional c-Si technology in mind. For high efficiency c-Si the philosophy does not change, except that care has to be taken to eliminate measurement artefacts due to measurement speed effects. Details [32] are beyond the scope of this paper, but recall that continuous light such as that provided outdoors enables measurement times around 1 s which are sufficiently slow to simulate steady-state conditions and eliminate any speed effects. As stated in section 3, the IV characteristics are measured from SC to OC conditions as this is less susceptible to sweep effects. However, the measurement systems allow a sweep in the reverse direction. For materials which are likely to have response time effects, sweeps in both directions are carried out, and sometimes a full analysis over a range of sweep speeds from 1 ms to 1 s is made. Only when this analysis shows that there are no effects due to the limited pulse duration on the LAPSSs, can modules be calibrated on these systems; otherwise the outdoor calibration is chosen. If the absence of sweep speed effects were not established, their presence would notably change the measurement result (in particular, the FF) and contribute significantly to the measurement uncertainty. Therefore, the present analysis is only valid in the absence of sweep speed effects.

For second-generation or thin-film PV modules, several calibration routes are possible. The calibration against a c-Si secondary reference cell is straightforward, but often has a large spectral mismatch. Suitably selected filtered c-Si secondary reference cells reduce the spectral mismatch while offering stability and can be used for common device technologies. However, there is always a remaining spectral mismatch leading to uncertainty. Alternatively, it is possible to calibrate a thin-film working reference device of the same technology as the module but with smaller size, eliminating the spectral mismatch between the module and the reference in actual calibration. Due to the smaller size this thin-film secondary reference can be calibrated on a CSS such as the Wacom with lower uncertainty than would be possible for the direct transfer from a c-Si reference to a module. As seen above, a secondary reference (filtered or not) has an uncertainty of $\pm 0.98\%$ (table 10). The transfer to a thin-film module yields $\pm 1.91\%$ for I_{sc} and $\pm 2.05\%$ for P_{max} . The thin-film working reference on the other hand could be calibrated with an uncertainty of $\pm 1.23\%$ (table 10). Using such a reference for the calibration of a thin-film module of the same technology the mismatch is eliminated and the overall uncertainty is $\pm 1.77\%$ for I_{sc} and $\pm 1.96\%$ for P_{max} , i.e. lower than the traditional route using c-Si references. Due to the inherent metastable behaviour of the thin-film devices, the working reference needs to be calibrated just before its use as a reference. This extra effort might be justified given the lower achievable uncertainty.

5.4. Improvements

A number of possible improvements and their importance are discussed in this section.

5.4.1. Data acquisition. The storage oscilloscope can be replaced by (three) digital voltmeters for slower data acquisitions (1 s) such as on the CSS Wacom and outdoor [33]. This reduces the electrical uncertainty (and system costs), but has limited impact on overall uncertainty as this contribution is negligible (figure 2). In the case of the calibration of the secondary reference cell of the same physical dimensions as the primary reference the optical uncertainty reduces and the electrical uncertainty starts to become the second most important contributor (after the primary reference cell).

5.4.2. Temperature control for the outdoor set-up. Outdoors the temperature uncertainty is the major contribution (60%). Therefore, even a modest improvement in temperature control would reduce the overall uncertainty. Hence, temperature control of the box so as to stabilize the module at the desired temperature (normally 25 °C) is envisaged for the near future.

5.4.3. Optical uncertainty—non-uniformity. For the LAPSSs the spatial non-uniformity is a significant contribution. In principle, it could be corrected for mathematically, but as the PV modules are series connected cells (with very different geometries for thin film and c-Si), this approach would be very tedious if not impossible. A reduction

of the non-uniformity through suitable optical components (filters, mirrors) might be possible, or the usage of a point source at ever longer distance which is, however, limited by lamp power. All these would require major changes, so that the outdoor set-up is the preferred solution since natural sunlight is perfectly uniform on the size of a single PV device for the short time of a measurement under clear sky conditions. The complexity of the required temperature control (see above) is less than that for improving existing simulators.

5.4.4. Spectral mismatch. The spectral mismatch can be reduced by better knowledge of the input variables, in particular the spectral irradiance of the (simulated) sunlight. This can be determined more easily and more accurately for continuous light sources, which are reflected in the lower uncertainty of the Wacom and outdoor. As already indicated above, another route is to use a small device of the same type as a reference and first calibrate this (taking advantage of the continuous light available easily for small size devices) and then use this device as a reference for large-scale modules eliminating spectral effects.

5.5. Stability issues

The stability of in particular thin-film PV modules is of concern. While this is important for a reliable correct measurement, it is not principally a problem of the measurement technology but rather the preconditioning of the device itself, which is beyond the scope of this paper.

5.6. Intercomparisons

Within the integrated project PERFORMANCE ESTI has participated in two round-robin exercises involving all major European PV testing laboratories. The first intercomparison [32] was carried out for high efficiency crystalline silicon modules and showed agreement between all laboratories within $\pm 2\%$ for maximum power determination and is hence consistent with tables 8 and 9. The second concerned thin-film modules [34] and resulted in a larger variation of measurement results. These could, however, be explained by other factors such as device instability and preconditioning, which have been excluded from the analysis here.

6. Conclusions

The traceability of PV device calibration and associated uncertainties for the ESTI measurement procedures has been presented so that the methodology can easily be adapted to set-ups in other laboratories. The major contribution is the reference cell uncertainty, which dominates for WPVS traceability and remains the main component (together with optical uncertainty) for direct traceability to the ESTI primary reference cell set. By introducing the latter the uncertainty in the calibration of the maximum power of PV modules is reduced from $\pm 2.6\%$ to below $\pm 2\%$.

For thin-film modules the calibration and use of a working reference of the same technology can help to reduce the overall

uncertainty as the spectral mismatch component becomes negligible in the actual calibration.

Further reductions in overall measurement uncertainty for the LAPSSs could be achieved by reducing the optical uncertainty. This would, however, require elaborate measures. Therefore, the outdoor set-up taking advantage of the uniformity of natural sunlight is preferred. As the temperature uncertainty is the major contributor to the overall uncertainty for the latter, the implementation of a temperature control system for the box in which the module is mounted would be beneficial.

Acknowledgments

This work was performed as part of the ESTI photovoltaic calibration ISO 17025 certification program. The assistance of the ESTI team, in particular Diego Pavanello, Alessandro Virtuani, Francesco Ponti, Francesco Merli and David Halton, was much appreciated. We thank Massimo Della Rossa (quality manager) and Ewan Dunlop (laboratory technical manager).

References

- [1] IEC 60904-4 2009 Photovoltaic devices: Part 4. Procedures for establishing the traceability of the calibration of photovoltaic reference devices 1st edn at press
- [2] IEC 60904-2 2007 Photovoltaic devices: Part 2. Requirements for reference solar devices 2nd edn
- [3] IEC 60904-1 2006 Photovoltaic devices: Part 1. Measurement of photovoltaic current-voltage characteristics 2nd edn
- [4] ISO/IEC Guide 98-3 2008 Uncertainty of measurement: Part 3. Guide to the expression of uncertainty in measurement (GUM: 1995)
- [5] ISO/IEC 17025-2005 2005 General requirements for competence of testing and calibration laboratories 2nd edn
- [6] Müllejjans H, Zaaïman W, Merli F, Dunlop E D and Ossenbrink H A 2005 Comparison of traceable calibration methods for primary photovoltaic reference cells *Prog. Photovolt., Res. Appl.* **13** 661–71
- [7] Müllejjans H, Zaaïman W, Dunlop E D and Ossenbrink H A 2005 Calibration of photovoltaic reference cells by global sunlight method *Metrologia* **42** 360–7
- [8] Müllejjans H, Ioannides A, Kenny R, Zaaïman W, Ossenbrink H A and Dunlop E D 2005 Spectral mismatch in calibration of photovoltaic reference devices by global sunlight method *Meas. Sci. Technol.* **16** 1250–4
- [9] Osterwald C R, Emery K A, Myers D R and Hart R E Primary reference cell calibrations at SERI: history and methods *Proc. 21st IEEE PVSC (Orlando, FL, 21–25 May 1990)* pp 1062–7
- [10] Zaaïman W, Müllejjans H, Dunlop E D and Ossenbrink H A 2006 SI traceability for irradiance transfer standards to silicon solar cells using direct and global irradiance *Proc. 21st Eur. PVSEC (Dresden, Germany)* pp 64–8
- [11] Finsterle W 2006 WMO International Pyrheliometer Comparison IPC-X 2005 *IOM Report No. 91* WMO/TD No. 1320, IMOD/WRC Internal Report, Davos, Switzerland
- [12] Fröhlich C 1991 History of Solar Radiometry and the World Radiometric Reference *Metrologia* **28** 111–5
- [13] Shimokawa R, Nagamine F, Miyake Y, Fujisawa K and Hamakawa Y 1987 Japanese indoor calibration method for the reference solar cell and comparison with outdoor calibration *Japan. J. Appl. Phys.* **26** 86–91
- [14] Walker J H, Saunders R D, Jackson J K and McSparron D A 1987 NBS measurement services: spectral irradiance calibrations *Natl Bur. Stand. (U.S.) Spec. Publ.* 250-20 102pp
- [15] Romero J, Fox N P and Fröhlich C 1995/96 Improved comparison of the World Radiometric Reference and the SI radiometric scale *Metrologia* **32** 523–4
- [16] Osterwald C R *et al* 1999 The world photovoltaic scale: an international reference cell calibration program *Prog. Photovolt., Res. Appl.* **7** 287–97
- [17] Osterwald C R *et al* 1998 The results of the PEP'93 intercomparison of reference cell calibrations and newer technology performance measurements: final report NREL/TP-520-23477 209pp
- [18] Emery K 2000 The results of the First World Photovoltaic Scale Recalibration NREL/TP-520-27942 14pp
- [19] ESTI laboratory accreditation by COFRAC 2-1671 (www.cofrac.fr)
- [20] ESTI quality system instruction I22-d 2008 Definition and use of ESTI reference cell set
- [21] Zaaïman W 1997 Simulator classification and performance verification: requirements for quality assurance programmes *Proc. 14th European PVSEC (Barcelona, Spain, 30 June–4 July 1997)* pp 2292–5
- [22] IEC 60904-7 2008 Photovoltaic devices: Part 7. Computation of the spectral mismatch correction for measurements of photovoltaic devices 3rd edn
- [23] IEC 60904-3 2008 Photovoltaic devices: Part 3. Measurement principles for terrestrial photovoltaic (PV) solar devices with reference spectral irradiance data 2nd edn
- [24] IEC 60891 1987 Procedures for temperature and irradiance corrections to measured *I–V* characteristics of crystalline silicon photovoltaic devices 1st edn
- [25] Bahrs U, Zaaïman W, Mertens M and Ossenbrink H A 1997 Automatic large area spectral response facility *Proc. 14th European PVSEC (Barcelona, Spain, 30 June–4 July 1997)* pp 2296–8
- [26] Ebner B, Agostinelli G and Dunlop E D 2000 Automated absolute spectral response characterisation for calibration of secondary standards *Proc. 16th European PVSEC (Glasgow, UK, 1–5 May 2000)* pp 1255–8
- [27] IEC 60904-8 1998 Photovoltaic devices: Part 8. Guidance for the measurement of spectral response of a photovoltaic (PV) device 2nd edn
- [28] ESTI quality system uncertainty calculation UC04 Spectral response and spectral mismatch factor with PASAN LAPSS LS-4
- [29] ESTI quality system uncertainty calculation UC42 Spectral responsivity with ORIEL CSS (SR)
- [30] Heidler K and Beier J 1988 Uncertainty analysis of PV efficiency measurements with a solar simulator: spectral mismatch, non-uniformity and other sources of error *Proc. 8th European Photovoltaic Solar Energy Conf. 1988 (Dordrecht: Kluwer)* vol 1 pp 554–9
- [31] Field H and Emery K 1993 An uncertainty analysis of the spectral correction factor *Proc. 23rd IEEE* pp 1180–7
- [32] Herrmann W, Mau S, Fabero F, Betts T, van der Borg N, Kiefer K, Friesen G and Zaaïman W 2007 Advanced intercomparison testing of PV modules in European test laboratories *Proc. 22nd European PVSEC (Milan, Italy, 3–7 Sept. 2007)* pp 2506–10
- [33] Ponti F 2008 Valutazione delle prestazioni di moduli fotovoltaici a film sottile e ad alta efficienza in condizioni outdoor *Thesis* Politecnico di Milano 196pp
- [34] Herrmann W, Zamini S, Fabero F, Betts T, Van Der Borg N, Kiefer K, Friesen G and Zaaïman W 2008 Results of the European PERFORMANCE project on the development of measurement techniques for thin-film PV modules *Proc. 23rd European PVSEC (Valencia, Spain, 1–5 Sept. 2008)* pp 2719–22